AUTOMATIC POSITION AND HEADING CONTROL OF A DRILLING VESSEL

by

A. W. Brink

J. B. van den Brug

C. Ton

R. Wahab

W. R. van Wijk

Paper to be presented at the
"Third Ship Control Systems Symposium",
26–28th September 1972, Bath, U.K.

September 1972

25740/4

INSTITUTE TNO for MECHANICAL CONSTRUCTIONS

P.O.Box 29, Delft, The Netherlands.

1. INTRODUCTION

The design of an automatic position and heading control system for a drilling vessel depends on the criteria, which must be satisfied by the vessel and its control system to perform its mission, on the environmental conditions in the area where the vessel will operate and on the expected behaviour of the vessel under these environmental conditions.

One criterion is that the safety of the crew and ship has to be ensured even in extremely adverse weather. A second criterion is that the vessel should have at least a specified number of workable days per year. Drilling operations have to be suspended if the bending of the drilling string exceeds a certain value. This limit is reached when the horizontal displacement of the vessel from the position, where the drilling string is vertical, is about 6 percent of the waterdepth.
The drilling vessel considered here is the "Pelican", built by the IHC-Holland ship yard "Gusto" for the French contractor Samaser. Main dimensions are: displacement 15.600 tons, length 137 m, beam 21.35 m and draft 7.32 m.

The vessel should be able to operate in waters of 50 - 300 m depth, under the following weather conditions: current speed 2 kt, wind speed 45 kt with gusts up to 65 kt and a sea with a mean period of 12 seconds and a significant wave height of 4.9 m.
To keep the vessel's motions, induced by current, wind and waves within the limits, the vessel is fitted with three variable pitch thrusters at the bow and two variable pitch thrusters at the stern and two variable pitch propellers. When proceeding at full power, using the propellers, the ship will attain a maximum forward speed of 13 kt.
The pitch of thrusters and propellers is controlled by an automatic position and heading control system, designed to reduce the measured position and heading errors. The position is measured by an acoustic device and the heading by a gyro-compass.

In the present project, the hull form, the number, location and maximum power of thrusters and propellers were fixed. The behaviour of the vessel with automatic control system was simulated on a hybrid computer. The simulation programme was used to obtain design data for the automatic control system, for investigating the behaviour of the vessel and control system under the specified environmental conditions and to improve the control system's effectiveness. The latter objective was achieved by investigating the effect of design parameter variation on the behaviour of the vessel and control system.

The simulation was based on a mathematical model describing the behaviour of vessel and control system. Necessary data for the mathematical model were determined by analytical computations and model experiments.

In the following section, a description will be given of the development and design of the automatic control system. Next the mathematical model is dealt with. In the last section the results obtained with the simulation are given.

2. AUTOMATIC CONTROL SYSTEM

2.1. Introductory remarks

The control system is part of a closed-loop system, schematically shown in figure 1.
The main components are:

- the measurement subsystem, including all devices for generating the information to be processed by the controller.
- the digital controller, of which the output is sent to the propulsors (main propellers and lateral thrusters) to control the pitch of the blades.

The ship is controlled in the horizontal plane: in the longitudinal (x) and lateral (y) direction and about the vertical z-axis (see figure 2). The main propellers are used to control the longitudinal motions, while the thrusters control both the lateral and the yawing motion about the z-axis.

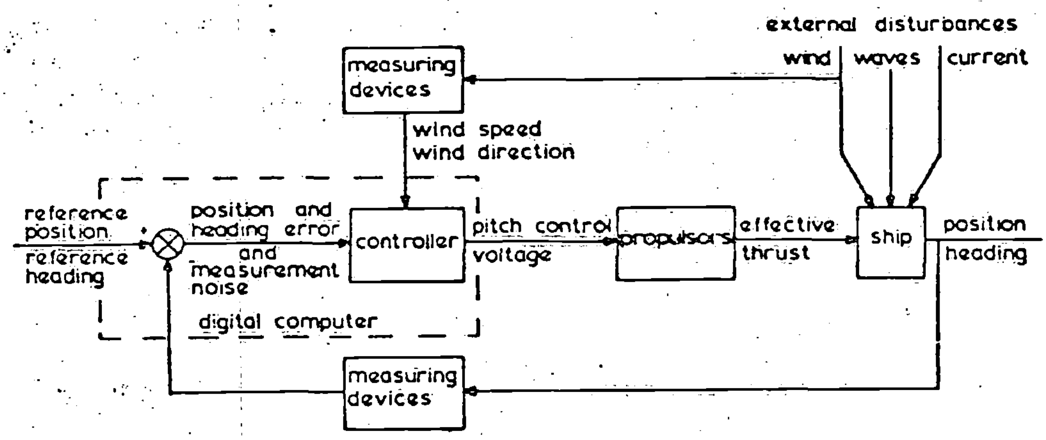

Figure 1. Block diagram of ship and control system.

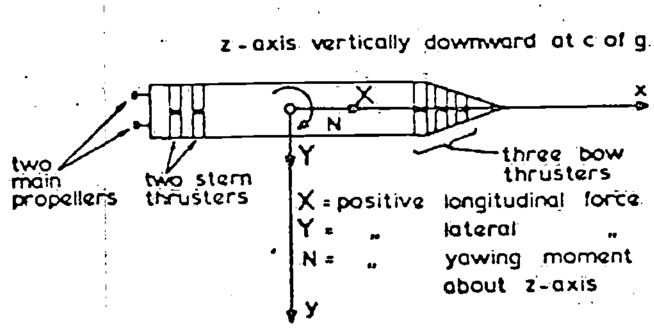

Figure 2. Thruster and propeller arrangement.

2.2. Requirements

During the actual drilling phase the automatic control system shall at least be capable of:

- controlling the propulsors for maintaining a reference-position and heading under specified adverse weather conditions, with a maximum allowable radial position error of 6 percent of waterdepth.
- avoiding high frequency fluctuations in the thrust demand ($\geq$ 0.05 cps), since this may cause unnecessary wear of the propulsors; moreover the power plant may not be capable to follow these fluctuations which may result in power interruptions.
- controlling the propulsors for changing the position or heading of the ship in case a new reference position or heading is selected.

The requirements with regard to the reliability of the system will not be discussed in this paper.

2.3. External disturbances

The motions of the vessel induced by the waves are oscillatory motions with frequencies equal to the wave frequencies. At the same time the vessel drifts off from its original position in the wave direction. Drift of the ship is also induced by the wind and the current.
The current speed and/or direction may be constant during a considerable period of time. If changes occur, in case of tidal currents, these changes are slow compared with fluctuations of wind speed, wind direction and wave forces.
The wind may be treated as a random Gaussian process of which the mean value is constant during a certain period of time. The frequency range in which the ship will respond to wind gusts is roughly between 0 - 0.04 cps.
The first-order oscillatory component of the wave forces is very large while the second-order component, the drift force is small. The motions of the ship induced by the first-order component are roughly in the frequency range between 0.05 - 0.25 cps, depending on the actual sea spectrum. These motions cannot be effectively counteracted because of the limited thrust of the propulsors.
The drift forces on the other hand are in the same frequency range as the responses due to the wind gusts.

Considering the requirements and environmental conditions, it may be stated that the control system should be designed to reduce the low frequency motions, while the relatively high frequency motions should be accepted without any counter measure.

2.4. Measurement subsystem

The primary sources of information are an acoustic position measurement device and the ship's gyrocompass.

The position error is obtained from the (short baseline) acoustic system, which consists basically of an on-board transmitter, a transponder on the seabed and four hydrophones mounted below the ship's hull. Upon interrogation by the transmitter (twice per second) the transponder answers, which signal is received by the hydrophones and after corrections for pitch and roll, translated into two digital signals indicating the longitudinal and lateral distance of the ship's centre of gravity relative to the transponder.
As the reference position, the well-head, does not coincide with the transponder, its position is also taken into account in order to calculate the position error relative to the reference position (see figure 3).

A heading error signal is obtained by comparing the actual heading with a chosen reference heading. The heading error is also available in digital form.

The wind speed and direction are measured and used to calculate the wind force acting on the ship for reasons explained in the next section. For this purpose sufficient data are available from wind tunnel tests.

At this place it must be mentioned that the signals received by the controller will be contaminated by measurement noise.

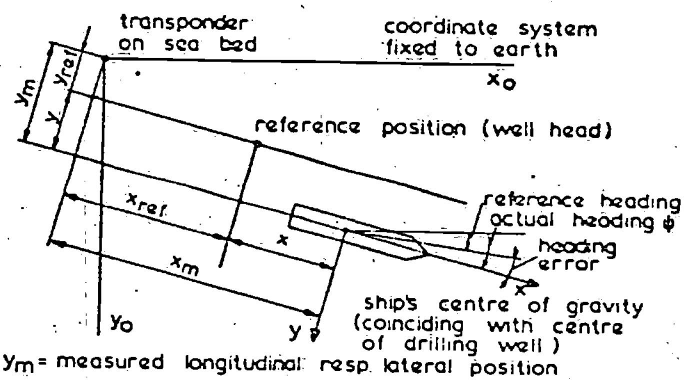

$x_m . y_m$ = measured longitudinal resp. lateral position
$x_{ref} . y_{ref}$ = reference position coordinates (depend on actual heading)
x , y = calculated longitudinal resp. lateral position-error

Figure 3. Axes system.

2.5. Controller

2.5.1. Basic ideas.

Keeping in mind the requirements mentioned earlier and the remarks made in section 2.3. some basic characteristics of the controller are formulated first. For this purpose the problem is reduced to the motions of a ship in only one direction, while the ship is considered to have a mass (M) and no damping. Non-linearities are not investigated in this phase. The transfer function of the uncontrolled ship is: (see also figure 4):

$$\frac{X(s)}{F_e(s)} = \frac{1/M}{s^2}$$

s being the Laplace transform operator and X(s), $F_e(s)$ being the Laplace transforms of the position x(t) and disturbing force $f_e(t)$ respectively.

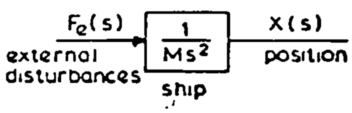

M: mass of ship, including "added" mass

Figure 4. Simplified block diagram of the uncontrolled ship.

Under sinusoidal steady state conditions we may write

$$\frac{X(j\omega)}{F_e(j\omega)} = -\frac{1/M}{\omega^2} .$$

It means that the magnitude varies proportional with ω^{-2}. It is obvious that the control system should improve the ship's behaviour only in the low frequency range. The actual range may be determined based on the remarks made in section 2.3., on the wind and drift force power spectra and on the allowable motion amplitude.

The transfer function of the controlled ship (see figure 5) is as far as the response to an external disturbance is concerned:

$$\frac{X(s)}{F_e(s)} = \frac{1/M}{s^2\ (1 + \frac{H_c H_t}{Ms^2})}$$

in which H_t is the transfer function of the propulsors and H_c represents the controller (which is assumed to be analog only for this initial study).

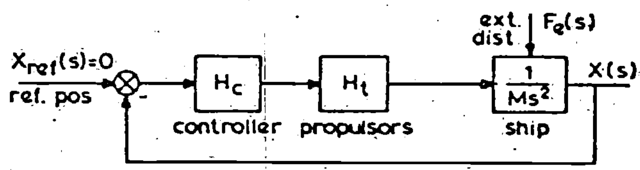

Figure 5. Simplified block diagram of the controlled ship.

Also

$$\frac{X(j\omega)}{Fe(j\omega)} = \frac{1}{-M\omega^2 + H_c(j\omega)\,H_t(j\omega)} .$$

Now consider the situation for $\omega \to 0$.
It is reasonable to suppose that $H_t \approx 1$ for $\omega \to 0$,
The magnitude

$$\left|\frac{X(j\omega)}{Fe(j\omega)}\right| \to \left|\frac{1}{H_c(j\omega)}\right| \quad \text{for } \omega \to 0.$$

From this it is concluded that $|H_c|$ must be made very large ($|H_c| >> 1$) in the very low frequency range in order to avoid "static" errors under constant external disturbances.
The gain level of the controller, which may be chosen in the frequency range between $\omega = 0$ and $\omega = 0.3$ rad/sec (≈ 0.05 cps), depends on the stability of the system. The stability is determined by constructing the Nyquist plot of the open loop transfer function:

$$H_{open}(s) = \frac{H_c(s)H_t(s)}{Ms^2}$$

and applying the Nyquist stability criterion. In particular the situation is determined relative to the (-1, 0) point (gain-margin, phase-margin), which is of particular importance when the response to command signals is investigated.
Also the ratio $\frac{1}{|1 + H_{open}|}$ as a function of ω is deduced from this plot.
Actually this ratio gives an indication about the effectiveness of the control system as far as the response to external disturbances is concerned:

$$\frac{X(s)_{controlled}}{X(s)_{uncontrolled}} = \frac{Ms^2}{Ms^2 \left(1 + \frac{H_c H_t}{Ms^2}\right)} = \frac{1}{1 + H_{open}} \; ;$$

thus

$$\left| \frac{X(j\omega)_{controlled}}{X(j\omega)_{uncontrolled}} \right| = \left| \frac{1}{1 + H_{open}} \right|_{s = j\omega} .$$

The foregoing deals with the steady state performance of the control system in response to sinusoidal inputs. It is also important to know the transient behaviour of the system. An insight can be obtained by solving the characteristic equation of the controlled system:

$$Ms^2 + H_c H_t = 0; \text{ in general: } H_c(s) = \frac{N_c(s)}{D_c(s)}, \quad H_t(s) = \frac{N_t(s)}{D_t(s)} \; ;$$

thus

$$Ms^2 D_c D_t + N_c N_t = 0, \text{ provided that } D_c \neq 0, D_t \neq 0.$$

The roots give an indication about the damping ratios, resonant frequencies and time constants. For an exact knowledge of the response to for example a unit impuls or unit step function also the numerators of the transfer function of the controlled ship should be taken into account.

In the previous part of this section, the controlled vessel was idealized to a linear system to deduce some basic characteristics. However, some of the neglected aspects are of prime importance:

- saturation of the propulsors may occur since the available power to generate thrust is limited
- the pitch rate of change of the propulsors is limited
- the motions are cross-coupled, e.g. a lateral motion causes a yawing moment and vice versa
- the developed thrust may deviate from the required thrust in many cases due to reasons, to be discussed later.

2.5.2. Wind feed forward.

It will be shown in section 4 that the wave induced "high frequency" motions alone may make up half of the allowable motions under certain conditions. Since this part cannot be reduced, severe limitations are imposed on motions due to wind and low frequency wave drift forces. To overcome this difficulty at least partially, wind feed forward compensation is used:
Wind speed and direction relative to the ship are measured. From this wind forces in x and y direction and the moment about the z-axis are calculated using wind tunnel test data. Pitch settings required to counteract these forces are deduced.
A revised schematic block diagram including wind feed forward is presented in figure 6.

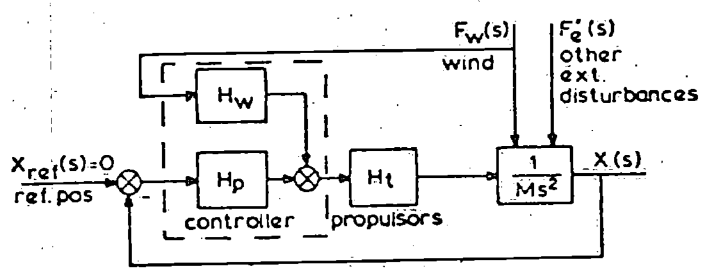

Figure 6. Simplified block diagram of the controlled ship, including wind feed forward.

We may write:

$$X(s) = \frac{{}^{1}/_{M}}{s^2} \frac{\left[1 + H_w H_t\right]}{\left[1 + \frac{H_p H_t}{Ms^2}\right]} F_w(s) + \frac{{}^{1}/_{M}}{s^2} \frac{1}{\left[1 + \frac{H_p H_t}{Ms^2}\right]} F_e^1 (s)$$

in which $H_w = \frac{F_{c_w}}{F_w}$ and F_{c_w} is the calculated force to counteract F_w;

$F_e^1 = F_e - F_w$.

If $H_w H_t = -1$ or $H_w = - \frac{1}{H_t}$ or $F_{c_w} = - \frac{F_w}{H_t}$ the influence of wind is reduced to zero.
For low frequencies, when $H_t \approx 1$, it is sufficient to make H_w as close to -1 as possible, depending on the accuracy of the wind meters and the wind tunnel data. A filter to suppress relatively high frequency components of the measured wind signal makes the feed forward compensation less effective.

2.5.3. Heading control priority.

During adverse weather conditions saturation of groups of propulsors may occur. A typical situation is given in figure 7.

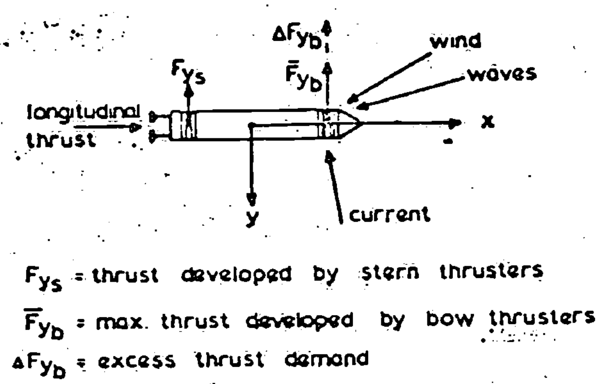

Figure 7. Example of saturation of propulsors.

Suppose that, due to a wind gust, the thrust demand at the bow exceeds the thruster capabilities. In that situation the ship is likely to make a large heading error away from the wind. If this happens the lateral wind force and moment increase even more as a result of which the ship is unable to hold its position. Obviously, such a situation should be avoided. This can be achieved by giving the heading control priority at the cost of position control.
If however the stern thrusters might saturate first in the same situation, the ship will head up into the wind, so that the lateral wind force and moment decrease. In that situation heading control priority is less useful, although rather large heading errors may occur, if priority is not given.

2.5.4. Controller.

The digital controller has roughly the following functions (see figure 8):
- filtering of the incoming position, heading error and wind information
- calculation of required thrust based on position and heading error information
- calculation of required thrust based on wind information
- calculation of required thrust per propeller and per thruster
- calculation of heading priority control if applicable
- calculation of the corresponding pitch control voltages for main propellers, stern and bow thrusters.

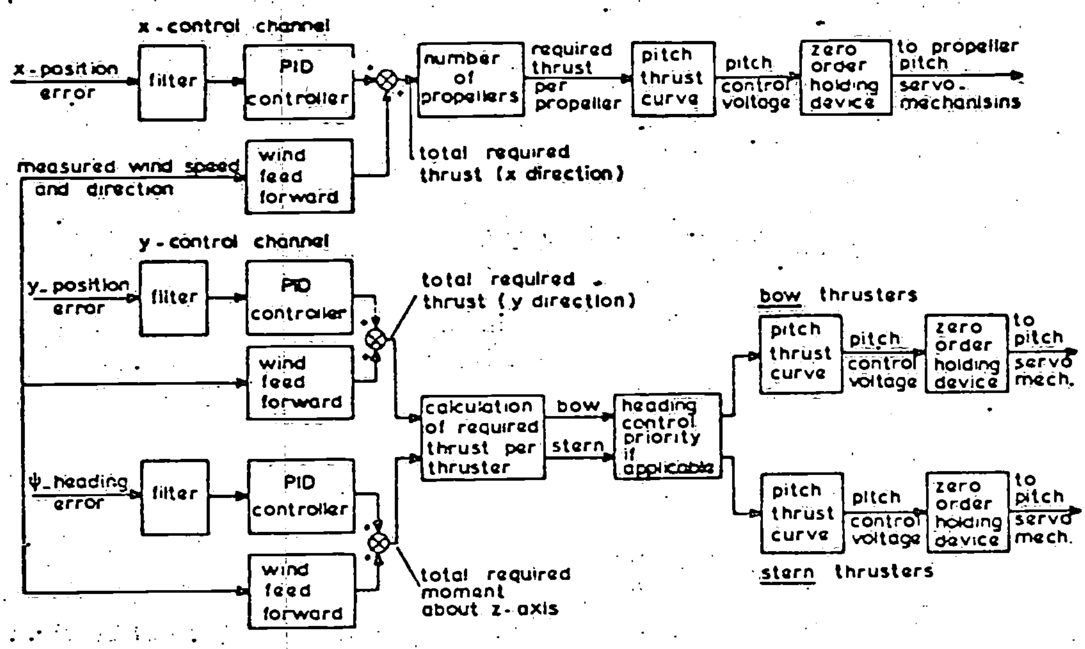

Figure 8. Block diagram of digital controller.

The acoustic position-error signals are received twice per second. This corresponds with a sampling frequency

$$\omega_s = \frac{2\pi}{0.5} \simeq 12.28 \text{ rad/sec.}$$

The computation-cycle time is made equal to the sampling period: T = 0.5 sec. Because the digital output is passed through a digital-analog converter, equivalent to a zero order hold circuit, which acts as a low pass filter, only signals with frequencies well below the sampling frequency are recovered.

Position- and heading error filters.

Figure 9 represents the shape of the ideal magnitude-curve of both the position and heading error filters. In this way both the high frequency wave motions and measurement noise are filtered out. Although a realizable filter may not follow this ideal curve, a close approximation is aimed at. A second very important requirement to be met is a small phase-shift in the low frequency range, since a phase-shift tends to make the system less stable. In practice a compromise between both requirements has to be accepted. The maximum phase-shift to be allowed can be determined using the methods described in the beginning of section 2.5. However, due to all simplifications only an approximation will be obtained.

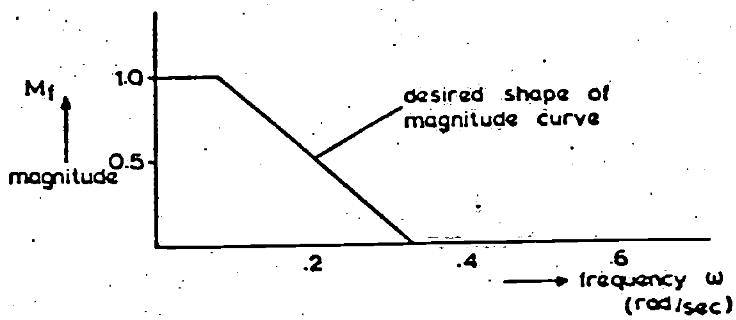

Figure 9. Magnitude versus frequency plot of filters.

The deviations from the "ideal" magnitude curve that can be tolerated, depend among other things on the noise level in the error signals, and last but not least on the basic PID-controller which is discussed in the next section.

PID-controller.

The second function (calculation of required thrust) is fulfilled by PID-controllers, one for each channel. In the frequency range of interest, all three may be considered to be "true three term" controllers. Although the actual controller is digital, the Laplace-transform is used to illustrate its behaviour:

$$\frac{F_x(s)}{X(s)} = K_x\left[1 + \frac{1}{\tau_{i_x} s} + \tau_{d_x} s\right]$$

in which: F_x = required force in x direction.

K_x = gain constant, τ_{i_x} and τ_{d_x} are time constants. It is shown that F_x consists of a part proportional with the position error itself, the integral value of the position error to cope with very low frequency disturbances and constant forces, and the derivative of the position error. The latter term introduces the necessary damping in the system.

From a stability point of view the integral time constant τ_i should be made as large as possible.

The actual value depends, however, also on the environmental conditions the system has to cope with, e.g. tidal currents.

Control "zones".

To improve the system it was decided to introduce control "zones" for control of the x and y motions.

These zones are defined as follows:

zone A : position errors $0 \leq |x| \leq x_A;\ 0 \leq |y| \leq y_A$

zone B : " " $x_A < |x| \leq x_B;\ y_A < |y| \leq y_B$

zone C : " " $|x| > x_B;\ |y| > y_B$

For each zone different gain and time constants may be used, but the integral term

$\frac{K_x}{\tau_{i_x}}$, resp. $\frac{K_y}{\tau_{i_y}}$ is kept constant in all zones.

The smallest values are used in zone A.
In zone B only τ_{d_x}, respectively τ_{d_y} is increased, while in zone C both K_x and τ_{d_x} (respectively K_y and τ_{d_y}) are increased.
Due to the low gain in zone A relatively large stability margins are guaranteed in the critical frequency range.
Once the ship moves out of zone A due to low frequency forces, the increased gain is used to oppose these motions, while at these lower frequencies still an acceptable stability margin is maintained.

z-Transfer functions of filters and PID-controllers.

For the actual design the z-transform technique has been employed. The z-transform is closely related to the Laplace-transform and is preferably used in case of digital control systems.
The general form of the z-transfer functions for the filters and PID-controllers is identical for all three control channels.

Filter:

$$H_{filter}(z) = K_f \frac{\prod_{k=0}^{M} (z-z_k)}{\prod_{k=0}^{N} (z-p_k)}$$

PID-controller :

$$H_{pid}(z) = K \left[1 + \frac{T}{2\tau_i} \frac{z+1}{z-1} + \frac{\tau_d}{T} \frac{z-1}{z} \right]$$

in which formula T denotes the sampling period (T = 0.5 sec). The second term in the latter formula denotes again the integral control action, while the third one represents the derivative control action.
The product of the two transfer functions yields the relationship between the required thrust (or moment) and the position (or heading) error.
For the x-channel it means :

$$\frac{F_x(z)}{X(z)} = H_{x_{filter}}(z) \cdot H_{x_{pid}}(z)$$

From these transfer functions the difference equations are deduced and used to program the computer.
The pole-zero configurations of the filters are initially determined before the simulation takes place. The same applies to the gain and time constants of the PID-controllers. The final configurations depend of course on the simulation findings.

Required thrust per propeller and thrusters.

The output of the PID-controllers plus the wind feed forward compensation represent the total required thrust in x and y direction and moment about the z-axis. The demand in x direction is evenly distributed between the two main propellers. The thrust required at bow and stern is determined in such a way that the lateral thrust does not create an unwanted moment and vice versa. In this procedure it is assumed that the thrust demand will be fully met. However, it has been stated already that a number of external factors make that the developed thrust is not equal to the demanded thrust.
One reason may be saturation of either the bow or the stern thrusters. In that case the controller initiates the heading priority-mode, the function of which has been explained earlier, and adjusts the thrust demand of both the bow and stern thrusters accordingly.
Once the required thrust per propeller and thruster has been calculated, the corresponding setting of the pitch of the propulsors is determined using manufacturer's thrust-pitch relationship data.

3. MATHEMATICAL MODEL

3.1. General

An important part of the mathematical model of the controlled vessel are the equations of motion of the ship. Their solution had to be anticipated to some extent in the set up of the model, which resulted in the block diagram of figure 10. The underlying idea of this set up is the assumption that the high and low frequency ship motions may be determined separately. Afterwords, the two types of motions are summed and the result is assumed to represent the motion of the ship in case both the high and low frequency exciting forces act on the ship at the same time. The high frequency motions are the linear wave induced ship motions, which take place with the wave frequency.. These motions are determined independently from the non-linear low frequency motions, which are caused by current, wind, thrusters, propellers and the wave induced drift forces. The separation of the high and low frequency motions is a consequence of the tools presently available for the determination of these motions.

A mathematical model of the vessel with automic control system can only be made if the characteristics of all its components are known.
However, the mathematical model is also a tool needed for determining the data necessary to design these components. This iteration process may eventually lead to an optimization of the complete system. In the following sections a brief description will be given of the principles used for the modelling of the components of the drilling vessel with automatic position and heading control.

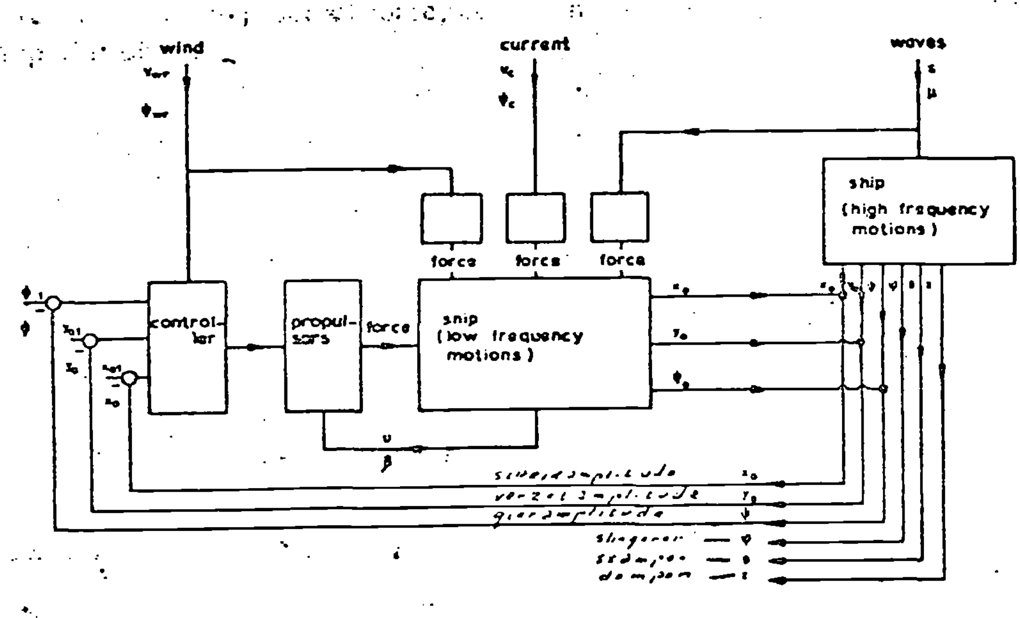

Figure 10. Block diagram of mathematical model

3.2. Low frequency ship motions

These motions are obtained by solving the equations of motion of the ship in the horizontal plane. The forces acting on the ship may be subdivided into:

- the hydrodynamic forces caused by the ship motions relative to the water
- the forces generated by the thrusters and propellers
- the wind forces
- the wave induced drift forces

Hydrodynamic forces.

The hydrodynamic forces in the horizontal plane are non-linear functions of the surge, sway and yaw motions of the ship; see figure 11 for definitions of the motions. These forces are analogous to those used for investigating ship manoeuvring as described in references [1] and [2].
A minor difference between the above forces and those acting on a manoeuvring ship is caused by the fact that in the present case the sway velocity may be large compared to the velocity in the surge direction.
For the present case the coefficients were estimated from measurements on ship models similar to the investigated one, supplemented with static tests with a captive model.

Thruster and propeller forces.

Propellers are used to generate the forces needed in the longitudinal direction of the vessel. A lateral force and a yawing moment may also be generated, however, in case of an oblique flow into the propeller. This force and moment may be large: in a 2 kt current the lateral force may amount to 20 to 55 percent of the longitudinal force, depending on the current direction and the propeller pitch.

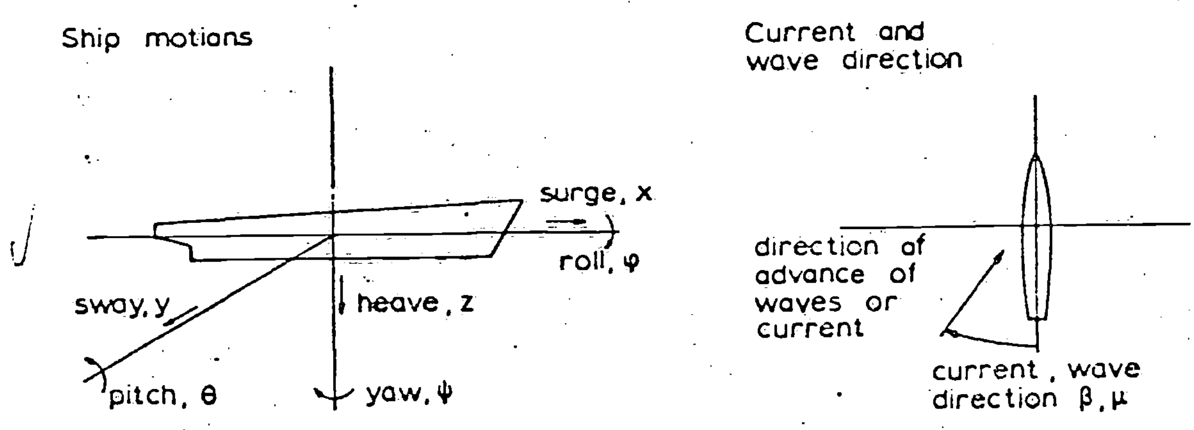

Figure 11. Definitions of the motions.

Also the developed thruster forces and moments are influenced by the current. This influence is illustrated for the bow thrusters in the figures 12, 13 and 14. Note in particular the large longitudinal force.
Interaction effects between the stern thrusters and the propellers add to the complexity of the system. The total lateral force generated by the thrusters does not only depend on the rpm and pitch of the thrusters, but also on the propeller thrust; variations of up to 30 percent of the nominal value occur. Vice versa, the thrust of the propellers is significantly influenced by the operation of the thrusters.
The mathematical model of the thruster and propeller forces generated by the propellers and thrusters includes the interactions and current effect mentioned above. The modelling was based on quantitative data obtained from an extensive series of model tests.

Wind forces.

Both the direction and magnitude of the wind speed change continuously in time. Of the instantaneous wind speed only the horizontal component is of interest. This horizontal wind speed is divided into a component in the average wind direction and a component perpendicular to this direction. Both components may be considered to be random variables, the latter one having a zero mean. Observations indicate that both components have a normal or Gauss probability distribution.

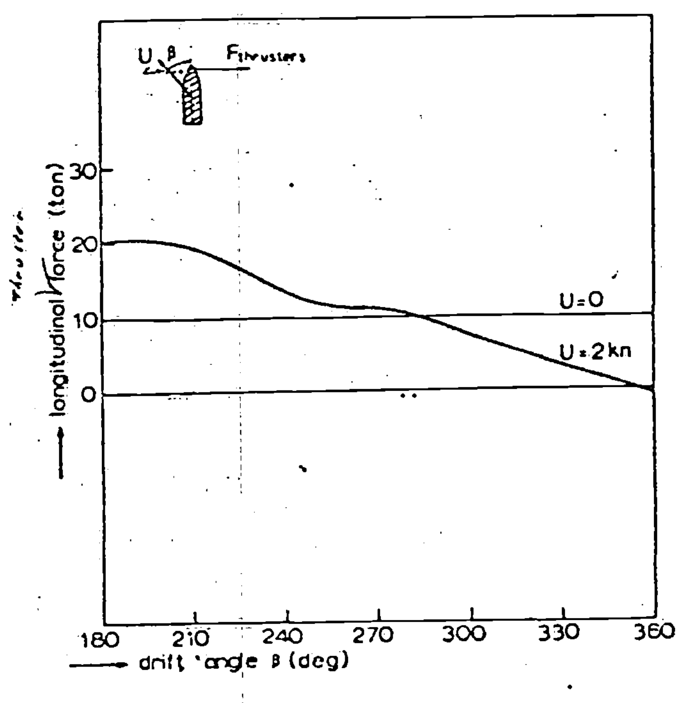

Figure 12. Longitudinal force verses drift angle.

Velocity U is relative to water.

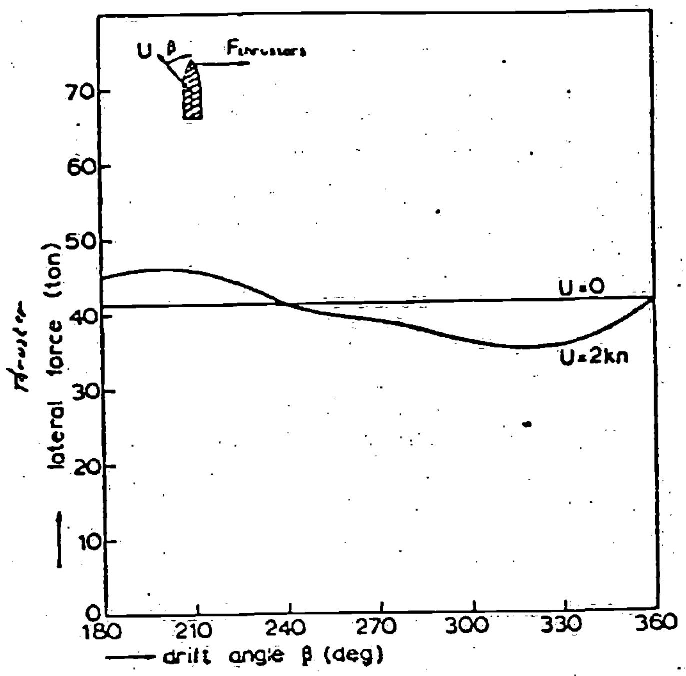

Figure 13. Lateral force versus drift angle.
Velocity U is relative to water.

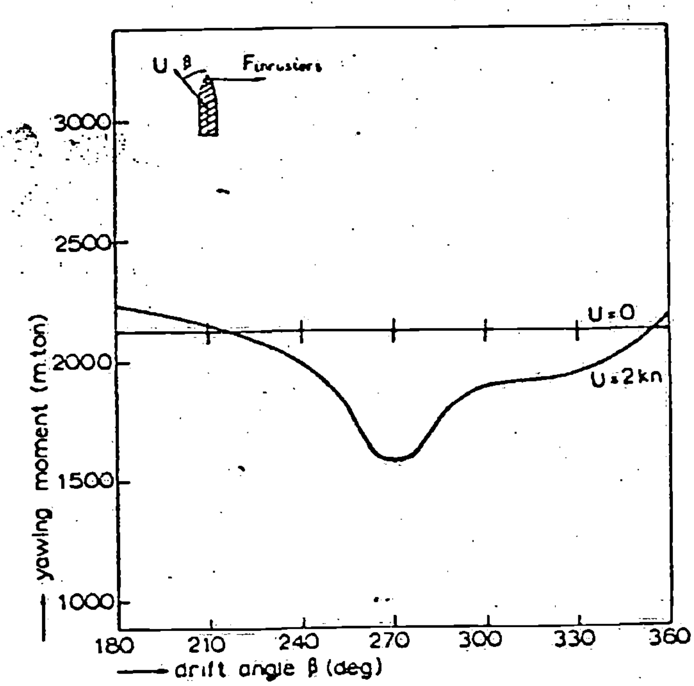

Figure 14. Yawing moment versus drift angle.
Velocity U is relative to water.

To set up a mathematical model of the wind variations the energy spectra of both components have to be known. Some information is available from literature [3] [4]. Using this information shaping filters are designed, that produce the desired random signals from a white-noise type input.
The wind induced forces and moments acting on the ship were determined by tests in a wind tunnel. Results for one wind speed are given in the figures 15, 16 and 17. The effect of the natural wind gradient was not measured in the tunnel, but instead determined from empirical formulas. Both methods give approximative results, because the actual wind gradient varies in time.
The measurements in the wind tunnel represent steady-state conditions, while as mentioned before in the real case the wind speed is not constant at all.
Yet in the simulation the wind forces and moment acting on the ship were calculated from the instantaneous wind speed and direction and using the wind tunnel measurements.
It is not known if this procedure introduces more than a negligible error.
Anyhow no other means are available to overcome this difficulty.

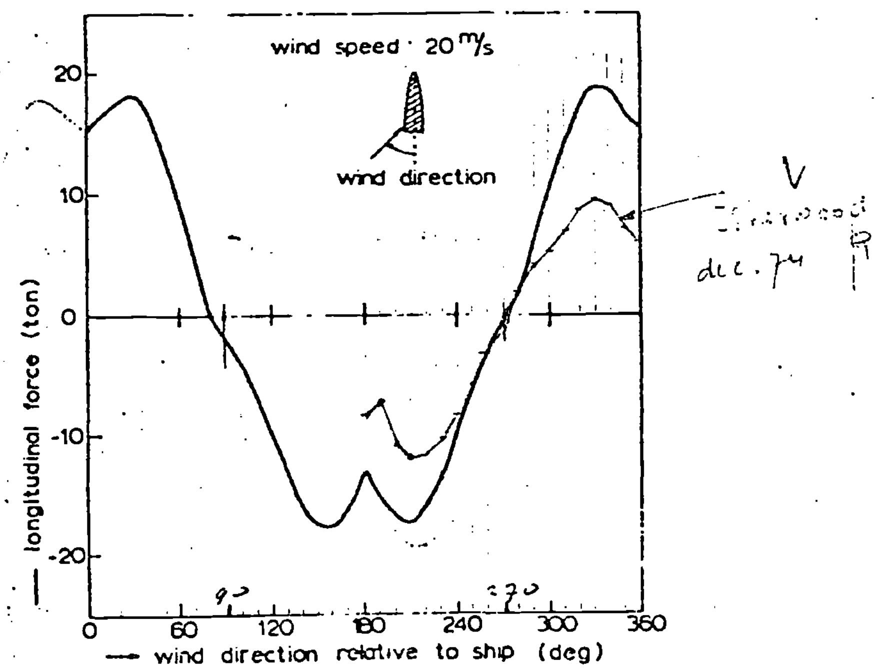

Figure 15. Longitudinal wind force versus relative wind direction.

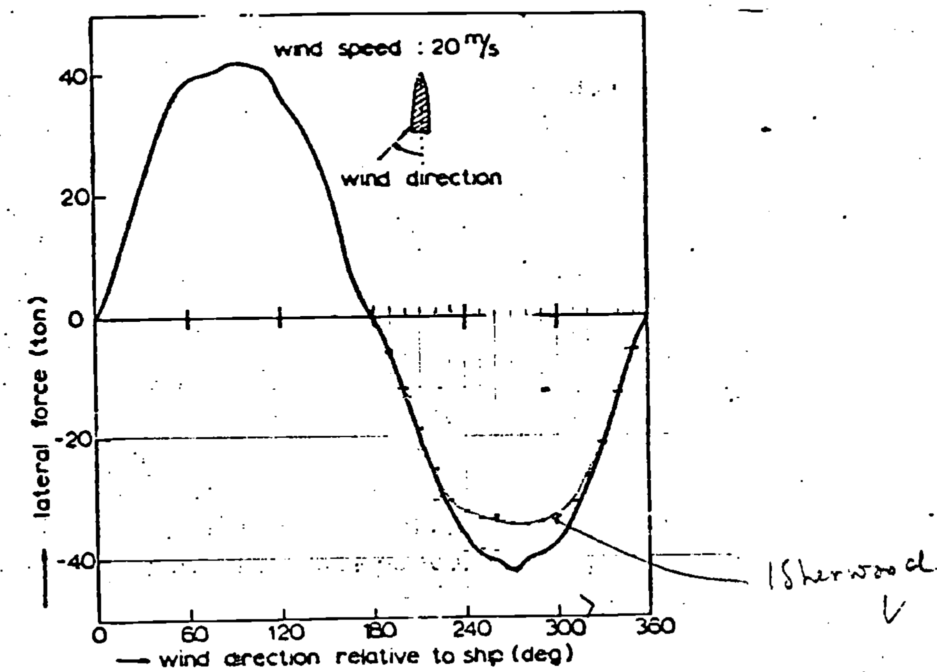

Figure 16. Lateral wind force versus relative wind direction.

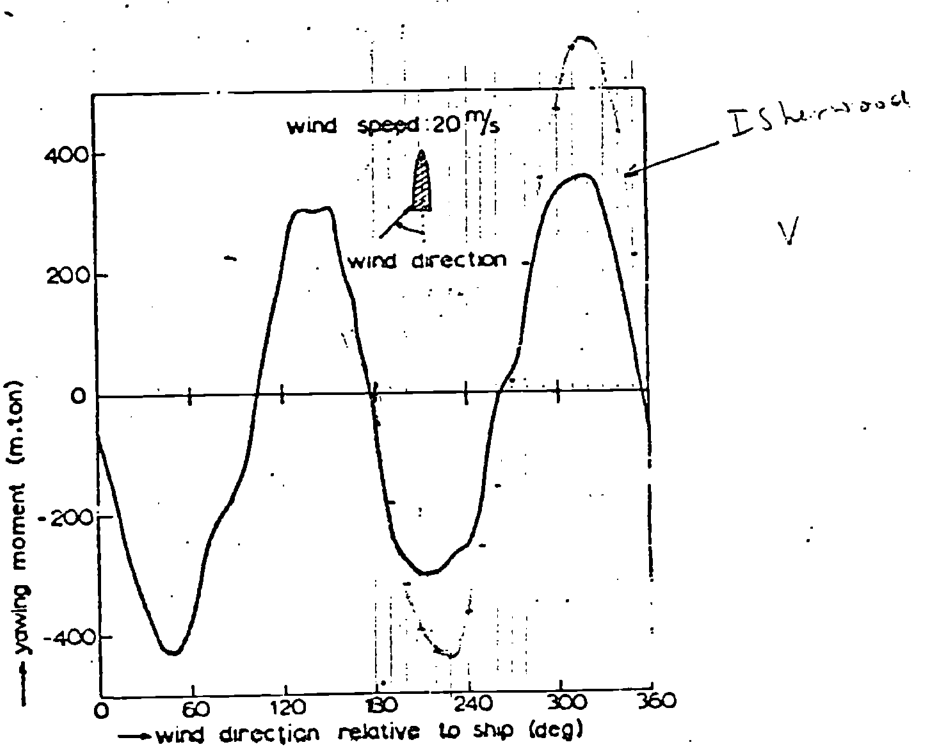

Figure 17. Yawing wind moment versus relative wind direction.

Wave induced drift forces.

These drift forces are calculated using a procedure described in reference [5]. It may be applied to a ship held fixed in space or to a vessel which is free to perform the high frequency wave induced motions in all six degrees of freedom. The figures 18 and 19 indicate the importance of these high frequency motions on the drift force and the drift moment. The magnitude of the drift force on a ship with position and heading control may be expected to lie between the values found for the captive and the free oscillating vessel, probably closer to the latter.
The drift force in irregular seas, which contrary to the regular wave case, varies in time, may be derived from regular wave data, following a procedure described in [6].
The figures 20 and 21 show the influence of the mean period of the sea on the mean value of the drift force and the drift moment. In these graphs the curves represent combinations of wave periods and heights most frequently found on the North Atlantic. The other investigated sea condition has the character of a swell.

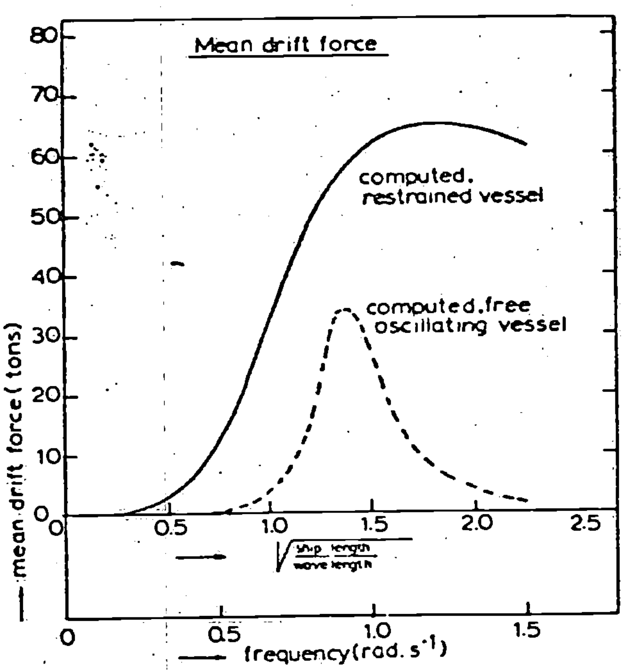

Figure 18. Mean drift force in regular beam seas with 1 m amplitude.

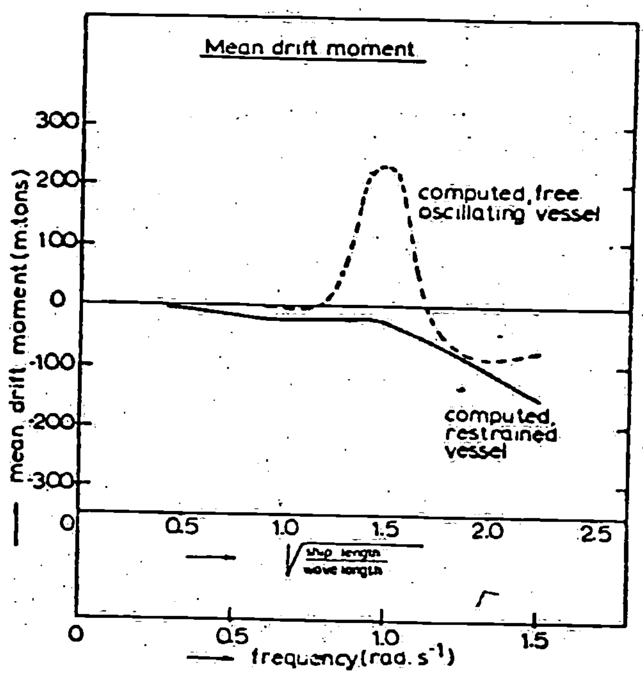

Figure 19. Mean drift moment in regular beam seas with 1 m amplitude.

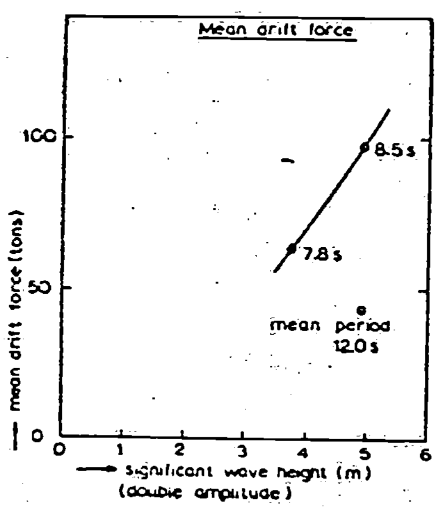

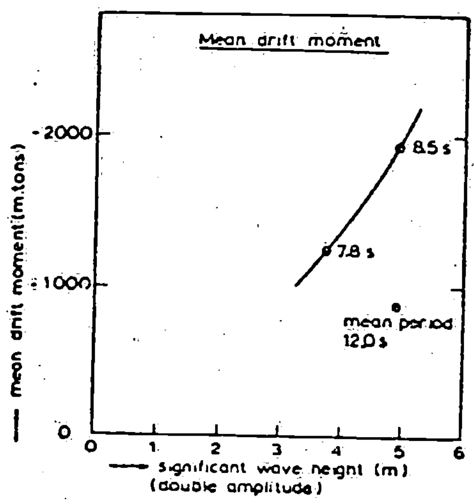

Figures 20 and 21. Influence of the mean period of a long-crested sea (wave direction 120 degrees) on the mean drift force and moment.

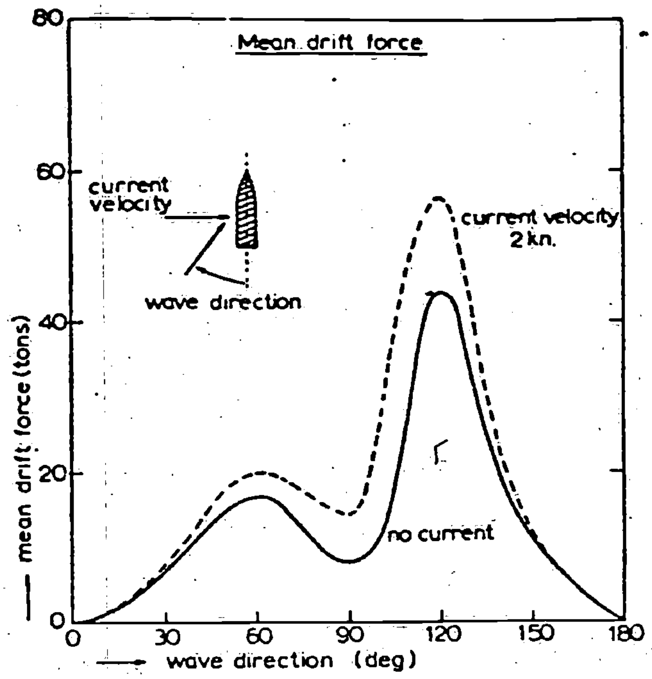

Figure 22. Influence of current and wave direction on the mean drift force in long-crested irregular seas.

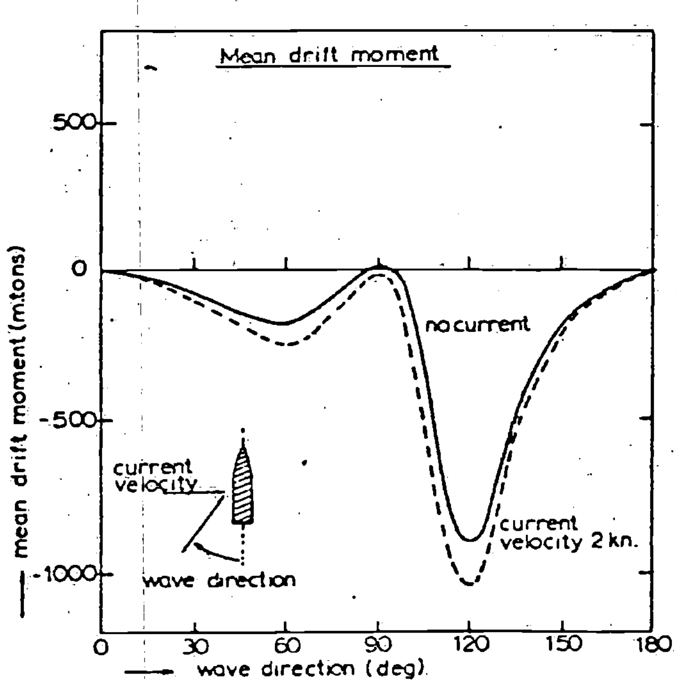

Figure 23. Influence of current and wave direction on the mean drift moment in long-crested irregular seas.

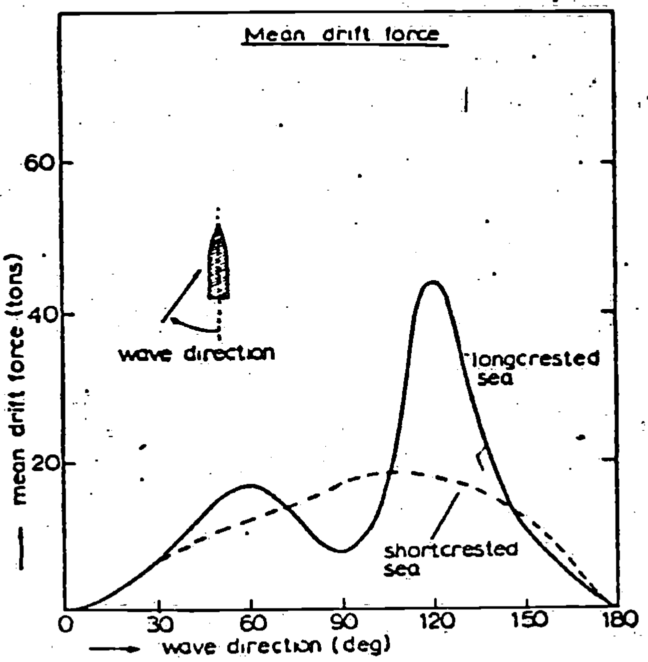

Figure 24. The drift force in short-crested and long-crested seas with the same significant wave height and mean period.

In the present calculations the effect of current on the drift force is taken into account by correcting for the changes in the frequency of encounter between the ship and the waves. Apart from this, it is assumed that the current does not affect the drift force. This approach may, on theoretical ground, raise objections. However, current speeds are small, and so is their effect on the motions. Although few experimental data were available for a validation, these data indicated that the approach used here yields acceptable results.

The figures 22 and 23 indicate that the largest drift forces and moments occur in bow seas. The marked difference between the forces in bow and quartering seas is caused by the asymmetry of the investigated vessel.
The irregular seas discussed above are long-crested. In reality the sea will be short-crested. Figure 24 shows the effect of the short-crestedness on the mean drift force. In the short-crested sea waves come from various directions over an angle of 180 degrees. The wave energy had a cosine squared distribution over this angle. In this case the wave direction is defined to be the direction of advance of the wave with the largest energy. In this study only long-crested seas are considered for simplicity reasons.

Summarizing, the equations of the low frequency ship motions are in the x and y direction and about the z-axis:

$$m(\dot{u}-rv) = X_{\dot{u}}\dot{u} + X_{vr}vr + X(U,\beta) + X_{wind}(V_{wr}, \psi_{wr}) +$$

$$+ X_{prop}\left(\left(\frac{P}{D}\right)_p, n_p, U, \beta, T_s\right) + X_{thr._s}\left(\left(\frac{P}{D}\right)_s, n_s, U, \beta, T_p\right) +$$

$$+ X_{thr._b}\left(\left(\frac{P}{D}\right)_b, n_b, U, \beta \right) + X_{waves}\left(\psi_{wa} - \psi, S_{\zeta\zeta}(\omega, U, \beta)\right)$$

$$m(\dot{v}+ru) = Y_{\dot{v}}\dot{v} + Y_{\dot{r}}\dot{r} + Y(U, \beta, r) + Y_{wind}(V_{wr}, \psi_{wr}) +$$

$$+ Y_{prop}\left(\left(\frac{P}{D}\right), n_p, U, \beta, T_s\right) + Y_{thr._s}\left(\left(\frac{P}{D}\right), n_s, U, \beta, T_p\right) +$$

$$+ Y_{thr._b}\left(\left(\frac{P}{D}\right)_b, n_b, U, \beta \right) + Y_{waves}\left(\psi_{wa} - \psi, S_{\zeta\zeta}(\omega, U, \beta)\right)$$

$$I_{zz}\dot{r} = N_{\dot{r}}\dot{r} + N_{\dot{v}}\dot{v} + N(U, \beta, r) + N_{wind}(V_{wr}, \psi_{wr}) +$$

$$+ N_{prop}\left(\left(\frac{P}{D}\right)_p, n_p, U, \beta, T_s\right) + N_{thr._s}\left(\left(\frac{P}{D}\right)_s, n_s, U, \beta, T_p\right) +$$

$$+ N_{thr._b}\left(\left(\frac{P}{D}\right)_b, n_b, U, \beta \right) + N_{waves}\left(\psi_{wa} - \psi, S_{\zeta\zeta}(\omega, U, \beta)\right)$$

3.3. High frequency ship motions

The high frequency ship motions were analytically determined from the equations of motion in six degrees of freedom of a ship proceeding in waves of an arbitrary direction. The six coupled linear differential equations used are given in reference [7]. The coefficients were determined from the two dimensional potential theory using strip method. A correction was applied to the roll damping, to take into account the viscous damping caused by bilge keels, in a manner described in the references [8] and [9]. For the computations, computer programmes were used which were developed by the Shipbuilding Laboratory of the Delft University of Technology. The motions in irregular seas were obtained from the regular wave behaviour using the linear superposition principle.

The effect of the thruster and propeller forces on the high frequency motions was neglected. This is justified, since the propeller and thruster forces are small compared to the high frequency hydrodynamic forces.
In beam waves of 1 m amplitude the exciting force amplitude may amount to 1400 tons, which is very large compared with the 75 tons maximum thrust generated by all thrusters combined.

3.4. The modelling of the propulsors

In case of variable pitch and constant rpm propulsors it may seem to be sufficient to introduce the operating characteristics of the pitch control system. In practice however, the rpm will not be constant due to the frequency variations of the electric power supply. A parallel simulation study was executed to determine if the amplitude of the rpm variation in operating conditions would show the necessity to include the power plant in the model of the total system.
In the present case the power is generated by a number of parallelled diesel generator units. The main loads on these diesels are the drilling operations and the electro motor driven propulsors. Peak loads are to be expected from the drilling operations and possibly from rapid pitch changes of the propulsors.
The mathematical model of the power plant including the loads, consists of the three parts

- the diesel generator units with rpm control.
- the electric motors of the propulsors and their loads.
- the electric load of the drilling equipment and main electrical system.

As a result of the study, the power plant was not included in the simulation of the total system.

It is of great importance that the pitch control system of the propulsors is included in the total system model, because the time lag between command signal and the resulting blade position has an unfavourable influence on the stability of the total system. The pitch control system is an electro-hydraulic servo system with an electro-mechanical pitch feedback. The system can be described adequately by a second order differential equation with a constraint on the rate of change of the pitch. The pitch control system of the thrusters is an on-off control with a dead zone and a load correction circuit.
The propeller pitch control system on the other hand is continuous.

3.5. Modelling of the control system

The functional description of the digital controller has already been given in section 2.5.
The computer, installed on board carries out a number of additional tasks in view of operational requirements. The controller as used in the simulation is a more or less simplified version, because it only fulfills the primary functions. One reason is that the main purpose of this simulation was to investigate the system performance under the most severe weather conditions. Under those conditions all propulsors and other components are assumed in operation.
The consequences of failure of one or more components has not been investigated.

Though it is advantageous to have the actual on-board computer available for the simulation this is not a necessity. However, the on-board computer and the simulation computer must have the same word length or the simulation computer must be programmed to have the same accuracy as the on-board computer.
The programme may be adapted and made more flexible for simulation purposes, because it must be possible to change parameters relatively easy and alter parts of the programme during the evaluation.

The acoustic measurement system was not simulated due to insufficient information. As an approximation, measurement noise was introduced with the measurement signals.

4. SIMULATION

4.1. Simulation programming

The simulation was performed on a EAI 690 hybrid system.
Figure 25 shows a detailed block diagram of the simulation set-up.
The low frequency equations of motion and the thruster and propeller servo systems and the thrust relations were programmed on the analog machine while using the digital machine for function generation.
The high frequency wave motions and the low frequency drift force variations were generated and stored on the disc as functions of time in advance and played back during the simulation runs.
The wind speed and direction variations were generated by noise generators with shaping filters. The position and heading were calculated digitally.
The simulations were performed at a time scale of 1 : 5, that means one hour in reality was simulated in 12 minutes.

The simulation program was used for:

- establishing the situations where propeller and thruster forces are in equilibrium with the mean current, wind and wave drift forces.
- determining the motions of the ship while assuming that the controller is capable of keeping the ship in the equilibrium position mentioned above and the ship only moves about the equilibrium position due to the high frequency wave forces.
- determining the motions in operating conditions.

4.2. Equilibrium positions

The equilibrium positions are determined for the situations where the thrusters and propellers operate with for instance 80 percent of the maximum pitch. The maximum thrust is not chosen to be able to cope with variations in the forces.
Figure 26 shows in which area's equilibrium is possible for combinations of wave and wind directions, for a certain sea state and a wind speed of 45 kt.
Figure 27 shows the influence of current, at one current speed (2 kt) but at variable direction, the sea and wind conditions are as before.
These results give a certain understanding of the capabilities of the drilling vessel. It must be mentioned however, that the variations in the acting forces may be considerably larger than the mean values. If for example the variations of the wave drift force are considered, the following can be stated.
Assuming the sea spectrum to be narrow, a common assumption, the lateral and logitudinal drift forces have exponential probability distributions with standard deviations equal to the mean. This implies that in 64 percent of the time the mean values are exceeded. A value exceeded only 5 percent of the time is three times the mean force. To which extend this results in too large motions will be determined later on.

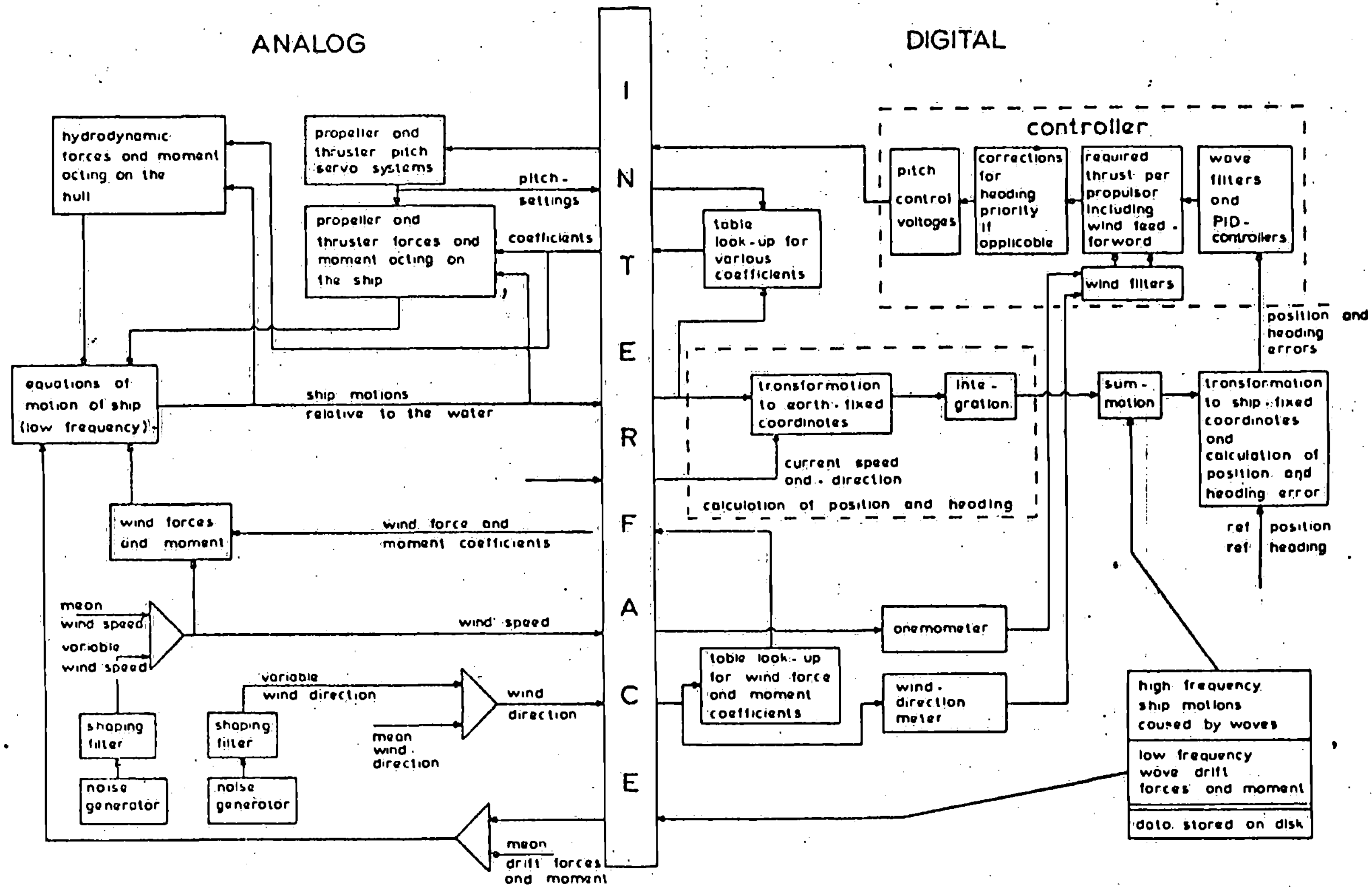

Figure 25. Block diagram of simulation.

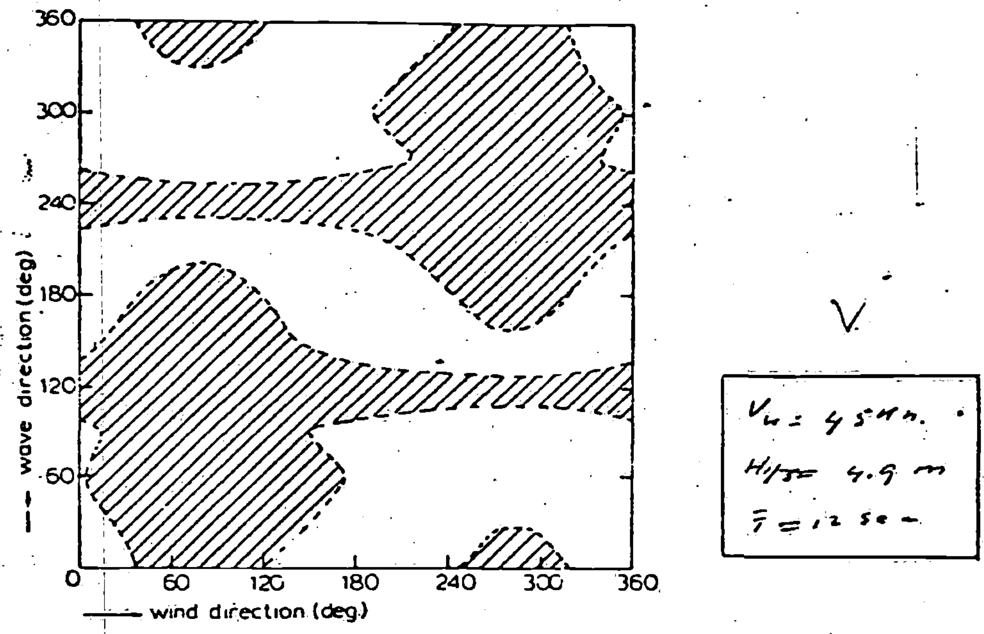

Figure 26. Equilibrium positions for various combinations of wind directions and wave directions. In the shaded area's equilibrium is not possible.

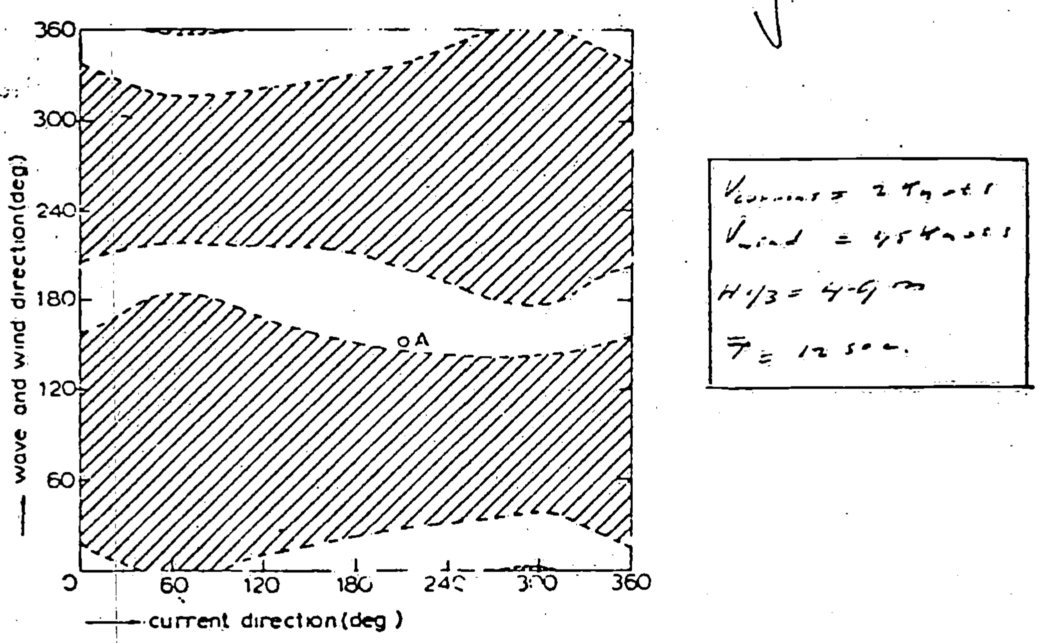

Figure 27. Equilibrium positions for various combinations of current directions and wave and wind directions. In the shaded area's equilibrium is not possible.

4.3. Motions in the wave frequency range

Comparison of the available thruster and propeller forces with the amplitudes of the oscillating part of the wave forces shows that it is impossible to counteract the oscillating ship motions induced by the waves. Therefore the controller should not react to motions of the wave frequencies, which is accomplished sufficiently by using wave filters. In the ideal situation when the thrusters and propellers are capable to cancel the low frequency forces continuously and the thrusters and propellers do not react to the position deviations caused by the high frequency wave forces, then these motions are the only motions performed by the ship. A better result can not be obtained. The motions in this situation were found by solving the set of equations for the mean equilibrium position with the earlier mentioned programme [7].

In figure 28, 29 and 30, the significant surge, sway and yaw motions (double amplitude) are shown as a function of the wave direction, in two irregular long-crested seas with an equal significant wave height of 4.9 m.

4.4. Motions in operating conditions

In the foregoing sections equilibrium positions in certain conditions were determined and motions in the wave frequency range were calculated, assuming an ideal control. In reality however, the ship will move as a result of the slow variation in wind, current and wave forces. In addition to that, ideal filters are not feasible and the controller will react to the ship motions in the wave frequency range. This does not affect the ship's motions, but among other things, leads to a lower effective thrust and to power modulation.
The simulations in this part had the objectives:

- to evaluate and if needed and possible, to improve the control system. The criteria are the position and heading errors, system stability and power modulation.
- to determine the capabilities in position keeping of the controlled ship in relation with the sea and weather conditions.
- to determine if the controlled ship can meet the required specifications of position keeping.

As an illustration, a part of a recording of a simulation run is shown in figure 31. The significant wave height was 4.9 m, the mean period 12 seconds, the wave direction was 150 degrees, the current speed 2 kt and the direction 210 degrees. The wind speed had a mean value of 45 kt, (Beaufort 9), gusting to 65 kt, while the direction varied within 20 degrees around 150 degrees. This situation is marked with an A in figure 27.

Recorded are channel 1 the radial position error (R), channel 2 the longitudinal position error (x), channel 3 the lateral position error (y), channel 4 the heading error (ψ), channels 5, 6 and 7 the pitch-diameter ratio of the propellers $(\frac{P}{D})_p$, bow thrusters $(\frac{P}{D})_b$ and stern thrusters $(\frac{P}{D})_s$, channel 8 the total power demand from propellers and thrusters N_t. One centimeter on the recording is equal to 50 seconds in reality.

From the recording it can be seen that although the equilibrium position is barely possible, the ship is able to keep position quite well under operating conditions with wave drift forces, wind speed and wind direction variations. The stern thrusters saturate from time to time and the propellers once on this part of the recording, but this did not lead to excessive position and heading errors.

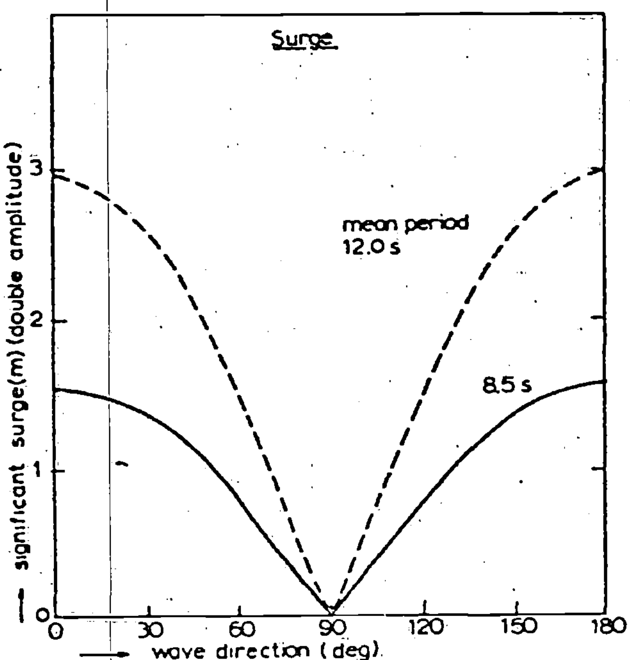

Figure 28. Influence of wave direction on the significant surge motion.

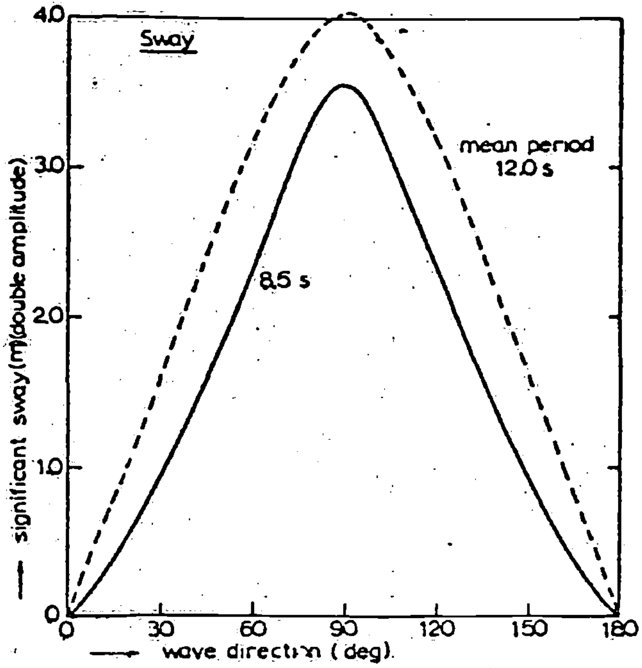

Figure 29. Influence of wave direction on the significant sway motion.

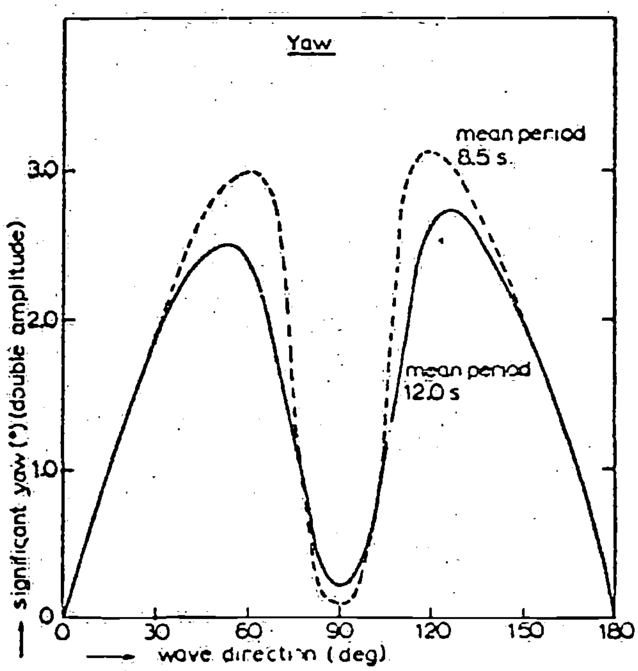

Figure 30. Influence of wave direction on the significant yaw motion.

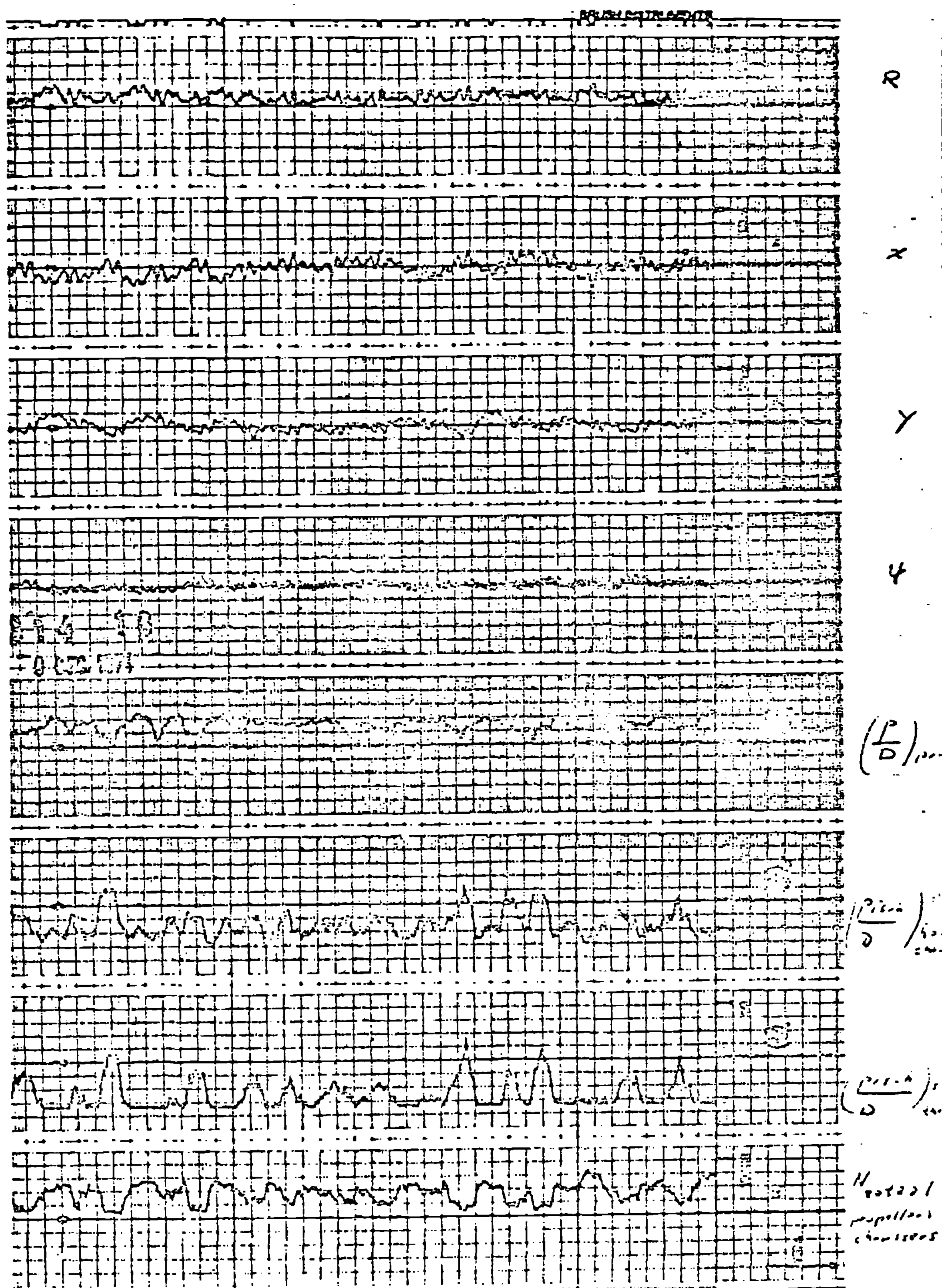

Figure 31. Typical recording of a simulation run.

5. FINAL REMARKS

In this paper it has been explained how in the design stage the behaviour of a drilling vessel with automatic position and heading control can be investigated by means of simulation.
The objective was to achieve design data for the control system and to investigate if the set criteria can be met in the given environmental conditions.
The agreement of the simulated process with the behaviour of ship and control system in reality depends on the exactness of the mathematical model.
Sea trials are necessary to determine the agreement of simulation results with reality. Results of these tests may indicate to which extent the mathematical model has to be improved.

The presented results are obtained from investigations by TNO-IWECO for the drilling vessel described in [10]. This ship was built by IHC-Holland for the contractor Somaser, Paris. The automatic control system was manufactured by Alcatel, Paris. The Alcatel design, which differs from the TNO-IWECO design, was also simulated by TNO-IWECO.
TNO-IWECO was assisted by IHC-Holland, the Netherlands Ship Research Centre TNO, the Shipbuilding Laboratory of the Delft University of Technology and the European Computation Centre of Electronic Associates Inc., Brussels. Model tests were performed at the Netherlands Ship Model Basin, Wageningen and at the Institut für Schiffbau der Universität Hamburg.

References

[1] Van Wijk, W.R. — Modelling of ships for simulation. TNO-IWECO report 8133/3, Delft, December 1970 (in Dutch)

[2] Brummer, G.M.A., C.C. Glansdorp, C.B. van de Voorde, W.R. van Wijk — Simulation of the Steering and Manoeuvring Characteristics of a Second Generation Container Ship. TNO-IWECO report 4829/2, Delft, to be published.

[3] Press, H., May T. Meadows, Ivan Hadlock — A Re-evaluation of Data on Atmospheric Turbulence and Airplane Gust Loads for Application in Spectral Calculations. NACA report 1272, U.S.A, 1956.

[4] Lumley, J.L., H.A. Panofsky — The Structure of Atmospheric Turbulence. Interscience Publishers, 1964.

* [5] Ogawa, A. — The Drifting Force and Moment on a Ship in Oblique Regular Waves. Shipbuilding Laboratory of the Delft University of Technology report 155, September 1966.

[6] Verhagen, J.H.G. — Low-frequency Drift Forces on a Drilling Vessel in Irregular Waves. Delft Hydraulic Laboratory report 637, November 1970 (not published).

[7] Vugts, J.H. — The Hydrodynamic Forces and Ship Motions in Waves. Thesis Delft University of Technology, 1970.

[8] Vossers, G. — Behaviour of Ships in Waves. Part C of Volume II (Resistance, Propulsion and Steering of Ships) in the series: Ships and Marine Engines, Stam, Haarlem, 1962.

[9] Tanaka, N., T. Hishida — A study on Bilge Keels. Journal of Zosen Kiokai, Parts 101, 103, 105 and 109 of August 1957, July 1958, July 1959 and July 1961.

[10] Sjouke, J., G. Lagers — Development of Dynamic Positioning for IHC Drill Ship. Paper presented at the Third Offshore Technology Conference, Dallas, Texas, 1971.

List of symbols

$f_e(t)$	external or disturbing force acting on ship (in the time domain)
$F_e(s)$	Laplace transform of $f_e(t)$
$F_w(s)$	Laplace transform of wind force
H	transfer function
I_{zz}	ship's moment of inertia
K	gain constant
m	ship's mass
M	total mass, i.e. ship's mass plus added mass
N	yawing moment about z-axis
N_{prop}	moment about z-axis developed by propellers
$N_{\dot{r}}$	added moment of inertia due to $\dot{r}$
N_t	power demand
N_{thr_b}, N_{thr_s}	moment about z-axis developed by bow and stern thrusters, respectively
$N_{\dot{v}}$	added moment of inertia due to $\dot{v}$
N_{waves}	low frequency wave drift moment about z-axis
N_{wind}	wind moment about z-axis
n_p, n_b, n_s	rpm of propellers, bow and stern thrusters, respectively
$(\frac{P}{D})_p, (\frac{P}{D})_b, (\frac{P}{D})_s$	pitch-diameter ratio of propeller, bow and stern thrusters, respectively
R	radial position error relative to well head
r, $\dot{r}$	yawing velocity and acceleration about z-axis, respectively
S	wave spectral density
s	Laplace transform operator
T	sampling period
T_p	nominal thrust developed by propellers
T_s	nominal thrust developed by stern thrusters
U	ship's velocity relative to the water
u, v	component of U in x and y direction, respectively
$\dot{u}$, $\dot{v}$	acceleration in x and y direction, respectively
V_c	current velocity, relative to the earth
V_{w_r}	wind velocity, relative to the ship

List of symbols (continued)

$X(s)$, $X(z)$	Laplace transform and z-transform of position error $x(t)$, respectively
X, Y	Force acting on ship in x and y direction, respectively
X_{prop}, Y_{prop}	Force developed by propellers in x and y direction, respectively
$X_{thr._b}$, $Y_{thr._b}$	Force developed by bow thrusters in x and y direction, respectively
$X_{thr._s}$, $Y_{thr._s}$	Force developed by stern thrusters in x and y direction, respectively
X_{waves}, Y_{waves}	low frequency wave drift force in x and y direction, respectively
X_{wind}, Y_{wind}	wind force in x and y direction, respectively
$X_{\dot{u}}$, $Y_{\dot{v}}$	added mass in x and y direction respectively
X_{vr}, Y_{vr}	added mass in x and y direction due to v and r
x, y, z	coordinate system fixed to the ship with origin in the ship's centre of gravity; also position error's in x, y and z direction
x_o, y_o, z_o	coordinate system, fixed to the earth
x_A, y_A, x_B, y_B	control zone-boundaries
z	z-transform operator
β	drift angle
θ, ϕ, ψ	pitch, roll and yaw angle
μ	wave direction relative to the ship
τ_d	time constant, used in derivative control equation
τ_i	time constant, used in integral control equation
ψ_c	current direction relative to the earth
ψ_{wa}	wave direction relative to the earth
ψ_{w_r}	wind direction relative to the ship
ω	frequency, radians per second
ω_s	sampling frequency, radians per second